Nanotechnology **21** (2010) 115301 (7pp) doi:10.1088/0957-4484/21/11/115301

Processing of loose carbon nanotubes into isolated, high density submicron channels

Troy R Hendricks[1], Ilia N Ivanov[2], Daniel A Schaeffer[1], Paul A Menchhofer[3] and John T Simpson[1]

[1] Measurement Science and Systems Engineering Division, Oak Ridge National Laboratory, Oak Ridge, TN, USA
[2] Center for Nanophase Materials Science, Oak Ridge National Laboratory, Oak Ridge, TN, USA
[3] Materials Science and Technology Division, Oak Ridge National Laboratory, Oak Ridge, TN, USA

E-mail: hendrickstr@ornl.gov and ivanovin@ornl.gov

Received 8 December 2009, in final form 11 January 2010
Published 22 February 2010
Online at stacks.iop.org/Nano/21/115301

Abstract
Loose multi-wall carbon nanotubes (MWNTs) were processed into a bundle of 19 600 individual channels with an individual channel diameter of 0.4 μm using a fiber drawing process. First, a powder of sodium silicate solution containing purified MWNTs was created. A glass capillary tube was filled with the powder and drawn into fibers. The fibers were cut into segments, bundled and redrawn multiple times to create fibers with multiple channels containing MWNTs. This processing approach created thousands of uniformly ordered channels containing dispersed MWNTs in a glass matrix while simultaneously aligning the MWNTs. The bulk resistivity of the MWNT-silicate channel has been improved by 38% after two consecutive draws as a result of the increased MWNT fraction.

(Some figures in this article are in colour only in the electronic version)

1. Introduction

The novel properties of carbon nanotubes (CNTs) have made them an attractive material for research and a future component in advanced multifunctional composites and novel electronic devices [1]. The high aspect ratio and crystallinity of the CNTs makes them an anisotropic conductor of heat and electricity on the scale of a single nanotube. Macroscopic samples of anisotropically conducting CNTs can be created by growing vertically aligned arrays of CNTs or applying shear forces to align CNTs in a composite [2–4]. Patterned growth of vertically aligned CNTs enables a design of electrically insulated CNT channels. The smallest feature size (produced via catalyst patterning) is limited to 2 μm due to the mechanism of CNT growth [4, 5]. Soft lithographically patterning the catalyst enabled growth of vertically aligned CNTs with 0.8 μm resolution [6]. Individually addressable vertically aligned carbon nanofibers have been grown in gated structures [7]. All of these approaches rely on the growth of the nanostructure on an electrode, and are limited by the CNT height. Other approaches to create single CNT fibers include processing CNT fibers by weaving [8], CNT processing from superacid [9] or forming polymer composites [10]. However, the smallest single fiber diameter obtained was around 200 μm by the superacid processed CNT. Extrusion and melt processing of CNTs in polymer matrix produces fibers with a diameter exceeding one hundred microns but is limited to low CNT loading due to the drastically increased density of the polymer [11, 12]. These approaches require additional processing steps to make electrically insulated bundles of these fibers and are currently limited by the fiber diameter to larger than a hundred microns. Processing loose CNTs into bundles of individually addressable conducting channels with a channel diameter less than a micron is technically challenging. These bundle assemblies of multiple conducting channels could be used as electrodes to spatially resolve intracellular species [13], chemically image analyte distribution near a surface [14] or for real-time detection of electrical and morphological changes of cells [15]. These conductive channel arrays can also be used to create neural prosthetic devices [16–18].

In this paper we demonstrate that glass fiber drawing technology could be used to process CNTs into multichannel

 © 2010 IOP Publishing Ltd Printed in the UK

assemblies. Glass fiber drawing, an existing industrial process that produces fiber optic cables, is a simple method to create nanosized structures with a controlled periodic structure [19, 20]. The fiber drawing process can be used for placing metallic and semiconducting materials in the fiber core to create micro- and nanowires [21, 22]. The process starts with a glass rod and tube which are drawn into fibers. The fiber is then cut into segments, bundled together and redrawn to produce fibers with an array of the core rod glass material. The bundling and drawing process can decrease the size of the material incorporated inside the tube to the nanoscale in only a few draws. Optionally, after the fiber segments are drawn they can be fused together and then cut into solid wafers with embedded nanostructures.

This paper outlines a modified fiber drawing technique used to simultaneously disperse and align loose multi-wall carbon nanotubes (MWNTs) into an array of submicron channels embedded in a glass matrix. The approach includes encapsulating the MWNTs in sodium silicate, drying the solution and grinding the MWNT–glass composite into a powder. A glass capillary tube is filled with the MWNT powder and drawn into fiber segments. The fiber segments are collected, bundled, placed in a glass tube and drawn again to further align and disperse the MWNTs in the glass matrix. With each draw the diameter of the MWNT-filled channels is reduced by a factor of 20 while the number of channels increases from a single channel (first draw) to 19 600 (third draw). Scanning electron microscopy (SEM), confocal laser microscopy, Raman spectroscopy and impedance spectroscopy were used to characterize the resulting glass fiber segments which contain thousands of channels embedded with MWNTs.

2. Experimental details

Figure 1 shows a schematic of the modified fiber drawing process. MWNTs were synthesized at the Oak Ridge National Laboratory by a CVD process employing ethanol as the carbon source and a nickel-based alloy in combination with a ferrous chloride sol as the catalysts. Raw multi-wall carbon nanotubes with an average length of 60 μm were purified by acid treatment in 30% HCl for 8 days at room temperature, followed by rinsing with DI water to a pH of 4. After purification, the MWNTs showed less than 2 wt% of the metal catalyst remaining. Fibers containing submicron channels of embedded MWNTs were created using a fiber drawing tower. Purified MWNTs were dispersed in a sodium silicate solution (J T Baker, ∼180 cps) to create a 0.1% solution which was tip-sonicated at a power of 300 W for 10 min. The encapsulation of MWNTs in sodium silicate has previously been demonstrated to coat MWNT fibers spun from vertical nanotube arrays [23]. After sonication the solution was heated in air at 550 °C for 4 h to remove the water from the sodium silicate. The remaining pieces of MWNT–sodium silicate glass were ground into powder using a mortar and pestle.

After the drying step, the powder was poured into a thick-walled Duran capillary tube (Schott North America, Inc., 9 mm OD 3 mm ID) which was sealed at one end. The capillary tube was heated in a vertical tube furnace under a partial vacuum at 700 °C for 4 h to remove residual water and minimize the formation of holes in the fibers during the drawing process. The tube was allowed to cool to room temperature and then was ready to be used as the preform for drawing. The preform containing the MWNT powder was heated in air to ∼900 °C until the preform started to draw into fibers. Once started, the fiber was drawn to a diameter of 0.46 mm using draw tower temperatures in the range 850–880 °C. A partial vacuum was applied to the preform during the drawing process to aid in collapsing the tube into a solid fiber. The fiber produced by the tower was cut into segments, bundled together and placed into a second thin-walled glass tube (9 mm OD, 1.5 mm wall thickness) to create a second preform. The second preform was drawn into fibers using the same temperature ranges, which resulted in fiber segments with an array of the original core material from the first draw (figure 2(a)). The double drawn fibers were then placed in a glass tube and drawn to create third drawn fibers. If even smaller channels are desired, the bundling and drawing process could be repeated again. The resulting fibers were characterized after each draw using a Hitachi S47000 field emission SEM, confocal laser scanning microscope (VK-9700, Keyence Corporation) and a Raman spectrometer (Renishaw, 633 nm). A Zahner IM6 impedance spectroscopy system with high impedance current and voltage probes was used to measure the electrical properties of the fibers in a two-electrode configuration with a frequency range of 0.1 Hz–1 MHz. For electrical measurements, a 2 cm long piece of the glass–CNT multichannel composite was painted with silver paste on both ends and contacted with IM6 using a two-pole configuration.

3. Results and discussion

The first draw of the preform containing the MWNT powder creates fibers with a single channel of MWNT down the middle as demonstrated in figure 2(a). The fibers produced in the first draw were bundled and drawn a second time, which results in fibers with a multichannel array of the original MWNT core material from the first draw. The bundling and drawing process was repeated which further dispersed the MWNTs, reduced the diameter of the original material and created thousands of channels with embedded MWNTs. Table 1 summarizes the fiber properties after each draw. Fiber segments from each draw were fractured at their end and observed with the SEM to analyze the alignment and dispersion of the MWNTs. The results are shown in figures 2(b)–(j). After the first draw, the MWNTs were embedded in glass along a single large continuous channel with a diameter of 150 μm. SEM images reveal that in this channel the sodium silicate creates a porous network where the MWNT phase separates from the silicate and occupies the voids, figures 2(c) and (d). We believe these voids are caused by a small amount of residual water vapor and air trapped in the loose packed sodium silicate powder. Investigation of the powder's weight loss upon heating in thermal gravimetric analysis experiments demonstrated that as much as 1 wt% of water was being released from the CNT-silicate powders. The sodium silicate melts at the drawing temperature and becomes too viscous to allow the trapped

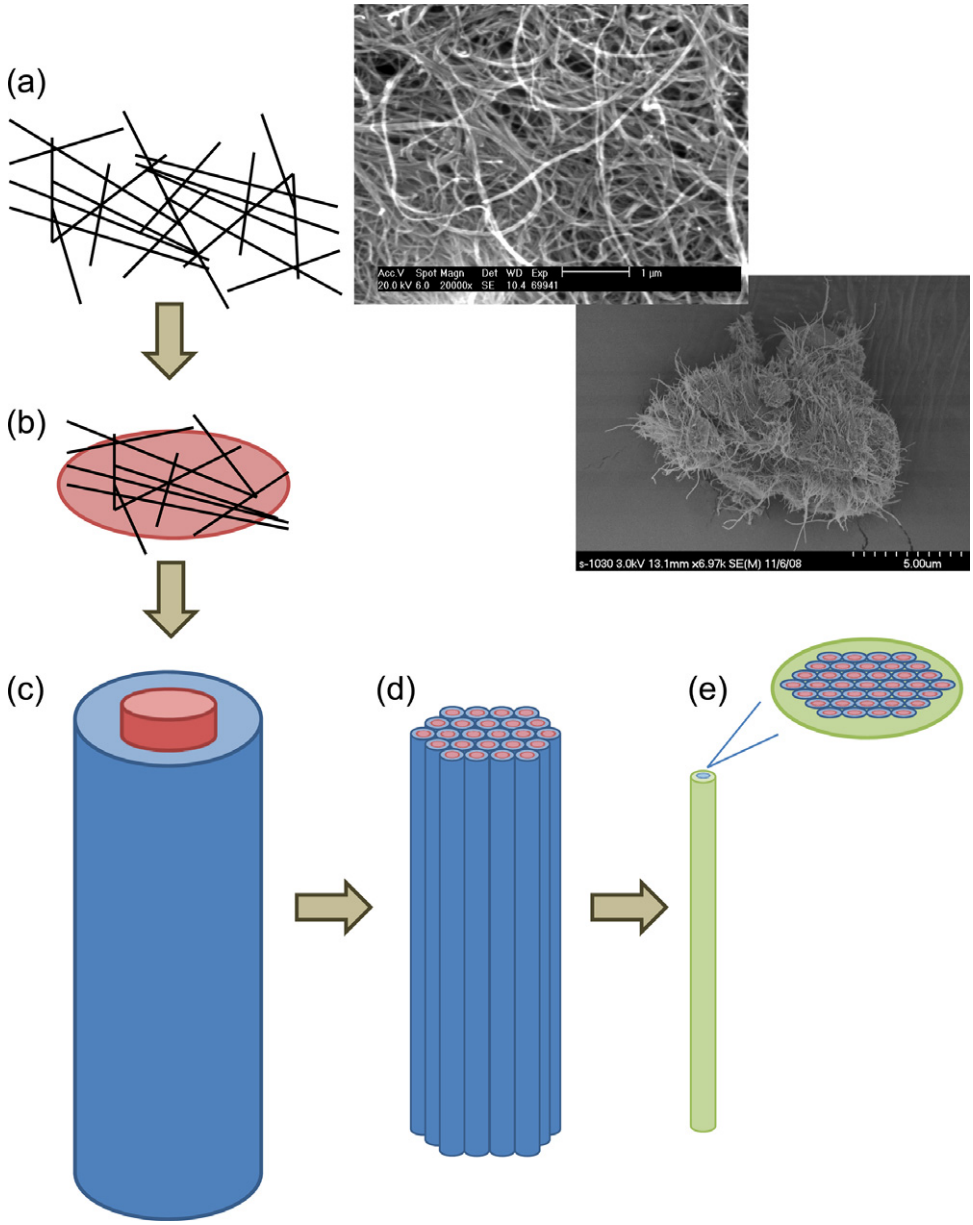

Figure 1. A schematic diagram of the modified fiber drawing process. MWNTs were synthesized by CVD (a). The MWNTs were encapsulated in sodium silicate, dried out and crushed into a powder (b). A glass capillary tube was filled with the MWNT-containing sodium silicate powder (c), drawn into fibers and cut into segments. The fiber segments were bundled together (d), placed in a second glass tube and drawn into fibers a second time. This resulted in a fiber with 140 channels containing MWNTs (e). The bundling and drawing steps ((d) and (e)) can be repeated to further decrease the diameter and increase the number of channels in the final fibers. The inset SEM images show the purified MWNTs and a MWNT–sodium silicate powder granule.

gasses to be removed by vacuum. The MWNTs observed in the voids of the single drawn fiber, figures 2(c) and (d), are still intertwined and observed in unaligned aggregates. However individual MWNTs can still be found on the fractured surfaces, figure 2(b).

After the first draw, the fiber segments are bundled and placed into a tube and drawn a second or third time. SEM images show the voids observed in the first draw fiber are almost completely collapsed after the second draw, and are completely closed after the third draw. In the second and third draw images, the ends of the multichannel fibers have lighter or darker regions where the MWNT density is greater. For instance, in figure 2(i) the dark spots represent the fiber produced in the second draw that contains 140 channels. The shear forces of the drawing process distributed and aligned the MWNTs along the fiber axis. Figure 2(b) shows an aggregate of unaligned MWNTs observed in a void in the sodium silicate-filled single channel. Figure 2(e) shows a 460 μm fiber from the first draw which was reduced to 22 μm with an 8 μm channel in the second draw. The MWNTs in the channel are aligned with the fiber axis and scattered around a region of the sodium silicate material. Figure 2(h) shows a close-up of a 140-channel second draw fiber that was reduced in size during the third draw. The channels were reduced to a

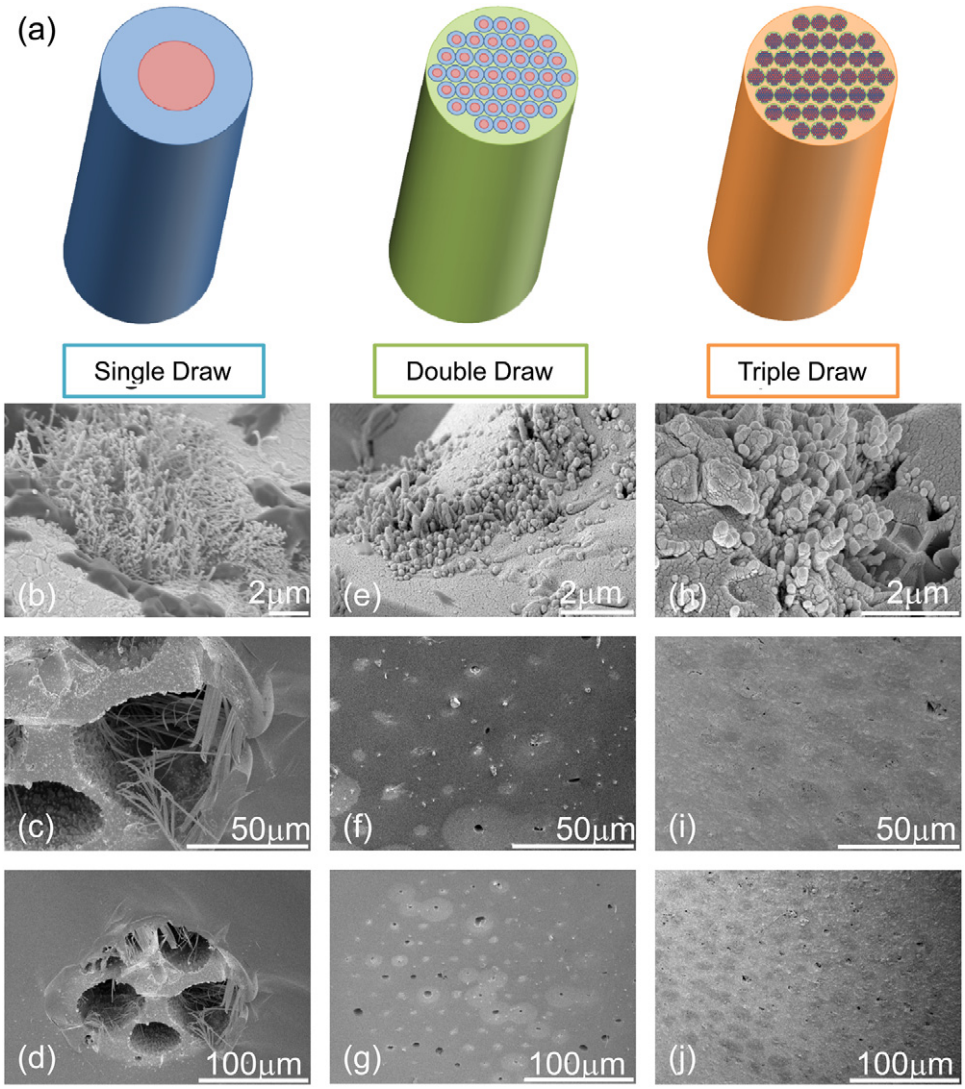

Figure 2. (a) A schematic diagram of the fiber ends after a single, double and triple draw. SEM images at different magnifications of MWNTs on the fracture surface of drawn fibers after consecutive draws, where ((b)–(d)) show a fiber produced after a single draw, ((e)–(g)) is a double drawn fiber and ((h)–(j)) is a triple drawn fiber.

Table 1. Summary of the multichannel fiber properties after each draw.

Draw type	Number of channels	Channel diameter (μm)	Channel resistance (GΩ)	Channel resistivity (Ω m)	Channel conductivity ($(\Omega\ \mathrm{m})^{-1}$)	Channel conductivity improvement (%)
Single	1	150	15	1.32×10^4	7.55×10^{-5}	
Double	140	7.67	4.20×10^3	9.70×10^3	1.03×10^{-4}	27
Triple	19 600	0.392	1.37×10^6	8.28×10^3	1.21×10^{-4}	38

diameter of 0.4 μm and the area where MNWTs are found was considerably smaller than the second draw fiber.

Confocal laser microscopy images were also utilized to study the distribution of the material in the drawn glass fibers. The images in figures 3(a) and (b) show that in the single draw fiber there is a central channel where MWNTs are embedded. The void regions in the sodium silicate are visible and appear discontinuous. The morphology of the sodium silicate inside the central channel of figure 3(a) is similar to the morphology observed in the single drawn fiber of figures 2(c) and (d). The MWNT aggregates and sodium silicate in the center channel appear unaligned with the axis of the fibers. Figures 3(d) and (e) are images of an MWNT-containing multichannel fiber after a second draw. The channels have a more uniform distribution of material than the single draw fiber. Furthermore, the MWNT aggregates and sodium silicate exhibited more order and are aligned axially down the length of the fiber. This reveals more evidence that MWNTs are being aligned through

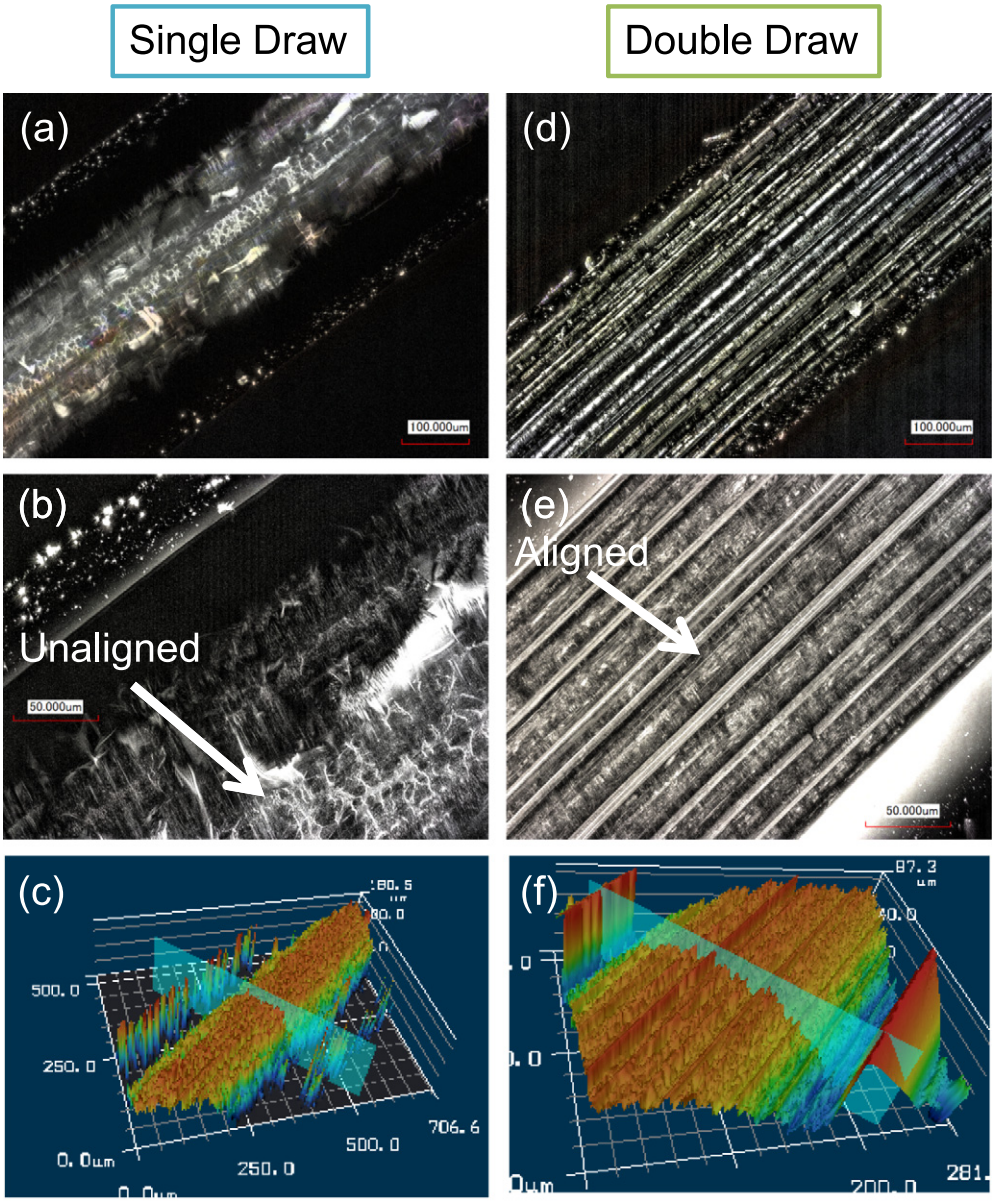

Figure 3. Confocal laser microscope images and 3D projections of ((a)–(c)) a single draw fiber and ((d)–(f)) double drawn fiber. These images demonstrate the change in alignment between the single and double drawn fibers.

the drawing process. The colored projections of the fibers, figures 3(c) and (f), are used to show the curvature of the 3D structure of the fiber that the previous images were taken from.

The MWNT integrity was characterized by observing changes in the Raman scattering spectrum through successive processing stages. The spectrum of pristine MWNTs in figure 4(a) exhibits characteristic bands of the tangential stretching G mode around 1580–1570 cm^{-1} and the double resonance feature around 1330 cm^{-1} (D mode) which is used as a measure of disorder that originates from defects or amorphous carbon [24]. The G′(D*) band observed around 2650 cm^{-1} as a second harmonic of the D band was also observed. Raman spectra of sodium silicate–MWNT sonicated and spin cast on a glass slide and MWNTs inside a second draw multichannel fiber were also obtained and are shown in figures 4(b) and (c), respectively. Both of these samples have the same characteristic D, G and G′ bands as the pristine MWNT sample. While quantitative characterization of the defects in MWNTs is difficult, the ratio of intensities of the D and G bands is usually used as a measure of disorder/defects in the sample [3]. The increase of the ratio between the D and G intensities indicates that the density of defects slightly increases during processing. The band structure in these measurements shows that the MWNTs survived the multi-drawing process.

The electrical properties of the multichannel MWNT–glass composite fibers were characterized using impedance spectroscopy, and the experimental results are shown in figure 5. The DC resistance of the fibers was obtained from the intercept of the semicircle and the real impedance axes at low frequencies. The first draw sample showed a DC resistance of around 15 GΩ. The second draw sample has

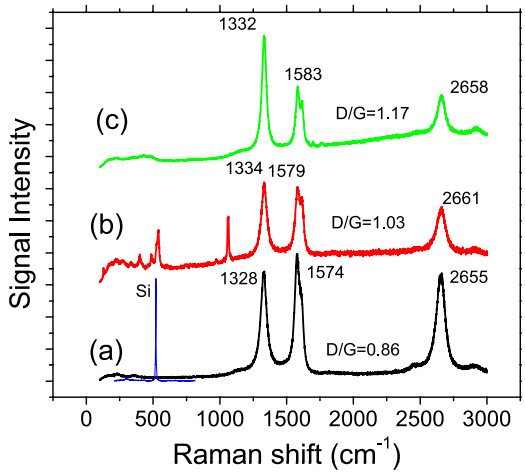

Figure 4. Raman scattering spectrum of MWNTs through the different processing stages. (a) Spectrum of pristine MWNTs. (b) Raman spectrum of Na silicate–MWNTs sonicated and spin cast on the glass. (c) Raman spectrum of MWNTs inside a second draw fiber. A 633 nm HeNe laser was used for excitation. The increase in the ratio of the D ($\sim$1330 cm^{-1}) and G (1580–1570 cm^{-1}) intensities suggests an increase in disorder through processing.

140 MWNT channels and shows a DC resistance of 30 GΩ. The third draw sample has 19 600 MWNT channels and a DC resistance of 70 GΩ. Assuming that individual channels have identical impedance values, and that during measurements all channels are short to form an equivalent circuit of individual impedances (Z_{ind}) connected in parallel, the impedance of an individual channel can be evaluated (figure 5(b)). The equivalent impedance of an MWNT–glass composite could be written as

$$Z_{\mathrm{eq}} = \frac{1}{n} Z_{\mathrm{ind}}$$

where n is the number of channels. In a low frequency approximation, the DC resistance of individual channels could be written as

$$R_{\mathrm{ind}} = n R_{\mathrm{eq}}.$$

The DC resistance of an individual channel after the first, second and third draw was estimated to be 15, 4.20×10^3 and 1.37×10^6 GΩ, respectively (table 1). The resistance (R) of an individual channel can also be expressed in terms of the silicate-CNT resistivity (ρ), channel cross section (A), channel diameter (d) and its length (L) as

$$R = \frac{\rho L}{A} = \frac{4\rho L}{\pi d^2}.$$

The resistivity of the individual channel, calculated using this equation, was found to decrease after each consecutive draw changing from 1.32×10^4 Ω m to 8.28×10^3 Ω m for the first and third draws respectively.

The conductivity of the individual channel, calculated as the inverse of the channel resistivity increases by 27 and 38% in the second and third draw, respectively, see table 1. The chemical nature of the material during the draw remains the same as indicated by Raman spectroscopy which showed no appreciable oxidation of the MWNTs. One possible reason for the improved bulk conductivity of the individual channels is the increased fraction of MWNTs as a result of bundled aggregate stretching. We also anticipate that silicate powder inside the channel would melt at the drawing temperatures and fuse into the glass while the MWNTs will remain inside the channel. This will also lead to an increase of MWNT fraction in MWNT-silicate material inside the channel. Establishing a concentration of MWNTs in the dispersant powder above the percolation threshold in the first draw sample is the key to obtaining high conductivity of multichannel MWNT–glass composites. This will be a target of our forthcoming experiments.

4. Conclusions

In summary, we were able to align and disperse MWNTs using a simple modified fiber drawing technique. The repeated drawing and bundling creates thousands of submicron channels containing MWNTs. The forces acting on the preform during drawing compress in plane and cause the MWNTs to distribute along the fiber axis. The alignment of the MWNTs reduced the channel resistivity by 38% in two consecutive draws. SEM and confocal laser microscopy verifies that these forces cause the intertwined MWNTs to align axially with the drawn

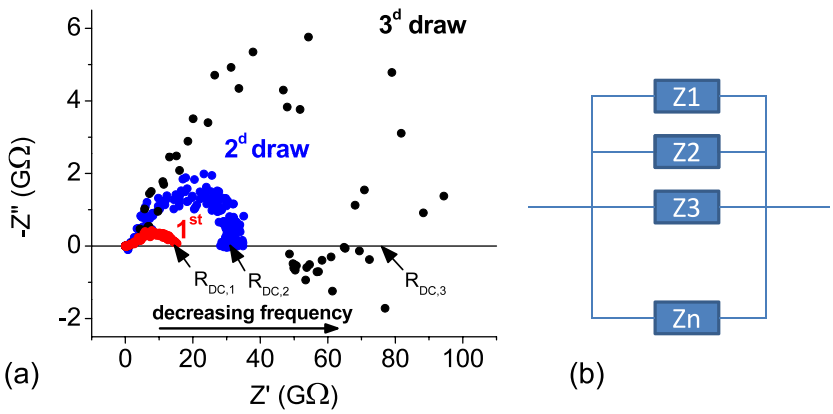

Figure 5. (a) Effect of the drawing process on the electrical impedance of 2 cm long pieces of MWNT–glass multichannel composite fibers. (b) The model of the equivalent circuit for a fiber with a multichannel array.

fibers. Raman confirms integrity of the MWNTs is maintained throughout the process. With future optimization, this process can be used to make thermal and electronically conducting multichannel assemblies for numerous types of biochemical devices.

Acknowledgments

This research was sponsored by the Laboratory Directed Research and Development Program of Oak Ridge National Laboratory (ORNL), managed by UT-Battelle, LLC for the US Department of Energy under contract no. DE-AC05-00OR22725. A portion of this research at Oak Ridge National Laboratory's Center for Nanophase Materials Sciences was sponsored by the Scientific User Facilities Division, Office of Basic Energy Sciences, US Department of Energy.

© Copyright US Government 2010

References

[1] Baughman R H, Zakhidov A A and de Heer W A 2002 Carbon nanotubes—the route toward applications *Science* **297** 787–92

[2] Andrews R, Jacques D, Rao A M, Rantell T, Derbyshire F, Chen Y, Chen J and Haddon R C 1999 Nanotube composite carbon fibers *Appl. Phys. Lett.* **75** 1329–31

[3] Ivanov I, Puretzky A, Eres G, Wang H, Pan Z W, Cui H T, Jin R Y, Howe J and Geohegan D B 2006 Fast and highly anisotropic thermal transport through vertically aligned carbon nanotube arrays *Appl. Phys. Lett.* **89** 223110

[4] Puretzky A A, Eres G, Rouleau C M, Ivanov I N and Geohegan D B 2008 Real-time imaging of vertically aligned carbon nanotube array growth kinetics *Nanotechnology* **19** 055605

[5] Wei B Q, Vajtai R, Jung Y, Ward J, Zhang R, Ramanath G and Ajayan P M 2002 Microfabrication technology: organized assembly of carbon nanotubes *Nature* **416** 495–6

[6] Huang S M, Mau A W H, Turney T W, White P A and Dai L M 2000 Patterned growth of well-aligned carbon nanotubes: a soft-lithographic approach *J. Phys. Chem.* B **104** 2193–6

[7] Guillorn M A, Melechko A V, Merkulov V I, Ellis E D, Britton C L, Simpson M L, Lowndes D H and Baylor L R 2001 Operation of a gated field emitter using an individual carbon nanofiber cathode *Appl. Phys. Lett.* **79** 3506–8

[8] Jiang K L, Li Q Q and Fan S S 2002 Nanotechnology: spinning continuous carbon nanotube yarns *Nature* **419** 801

[9] Ericson L M *et al* 2004 Macroscopic, neat, single-walled carbon nanotube fibers *Science* **305** 1447–50

[10] Vigolo B, Penicaud A, Coulon C, Sauder C, Pailler R, Journet C, Bernier P and Poulin P 2000 Macroscopic fibers and ribbons of oriented carbon nanotubes *Science* **290** 1331–4

[11] Haggenmueller R, Gommans H H, Rinzler A G, Fischer J E and Winey K I 2000 Aligned single-wall carbon nanotubes in composites by melt processing methods *Chem. Phys. Lett.* **330** 219–25

[12] Thostenson E T and Chou T W 2002 Aligned multi-walled carbon nanotube-reinforced composites: processing and mechanical characterization *J. Phys. D: Appl. Phys.* **35** L77–80

[13] Meulemans A, Poulain B, Baux G, Tauc L and Henzel D 1986 Micro carbon electrode for intracellular voltammetry *Anal. Chem.* **58** 2088–91

[14] Schrock D S and Baur J E 2007 Chemical imaging with combined fast-scan cyclic voltammetry-scanning electrochemical microscopy *Anal. Chem.* **79** 7053–61

[15] Liebetrau J M, Miller H M and Baur J E 2003 Scanning electrochemical microscopy of model neurons: imaging and real-time detection of morphological changes *Anal. Chem.* **75** 563–71

[16] Rubinstein J T and Miller C A 1999 How do cochlear prostheses work? *Curr. Opin. Neurobiol.* **9** 399–404

[17] Loeb G E, Wilson B S and Larry R S 2009 *Encyclopedia of Neuroscience* (Oxford: Academic) pp 1051–4

[18] Richter C-P, Fishman A J and Izzo A D 2008 Cochlear nerve stimulation with optical radiation *Otolaryngol.—Head Neck Surg.* **139** P99

[19] Tonucci R J, Justus B L, Campillo A J and Ford C E 1992 Nanochanel array glass *Science* **258** 783–5

[20] D'Urso B, Simpson J T and Kalyanaraman M 2007 Nanocone array glass *J. Micromech. Microeng.* **17** 717–21

[21] Zhang X J, Ma Z Y, Yuan Z Y and Su M 2008 Mass-productions of vertically aligned extremely long metallic micro/nanowires using fiber drawing nanomanufacturing *Adv. Mater.* **20** 1310–4

[22] Hong Y, Ma Z Y, Wang C M, Ma L Y and Su M 2009 3D ordered assemblies of semiconductive micro/nanowires using microscale fibrous building blocks *ACS Appl. Mater. Interfaces* **1** 251–6

[23] Peng H, Jain M, Peterson D E, Zhu Y and Jia Q 2008 Composite carbon nanotube/silica fibers with improved mechanical strengths and electrical conductivities *Small* **4** 1964–7

[24] Rasheed A, Dadmun M D, Ivanov I, Britt P F and Geohegan D B 2006 Improving dispersion of single-walled carbon nanotubes in a polymer matrix using specific interactions *Chem. Mater.* **18** 3513–22